Spatially organized lymphocytic microenvironments in high-grade primary prostate cancer

Jeremiah Wala[1,†], Ali Amiryousefi[2,3,†], Jia-Ren Lin[2,3], Brian William Labadie[4], Aishwarya Atmakuri[4], Eamon Toye[4], Kiranj Chaudagar[4], Madeleine S. Torcasso[4], Shannon Coy[2,5], Giuseppe Nicolo Fanelli[6,7], Brigette Kobs[2,3], Fabio Socciarelli[6], Andreanne Gagne[8], Eliezer M. Van Allen[1], Peter Sorger[2,3,*] & Akash Patnaik[4,*]

[1]Dana Farber Cancer Institute, Boston, MA 02215, USA
[2]Laboratory of Systems Pharmacology, Department of Systems Biology, Harvard Medical School, Boston, MA 02115, USA
[3]Ludwig Center at Harvard, Harvard Medical School, Boston, MA 02115, USA
[4]Section of Hematology/Oncology, Department of Medicine, University of Chicago, Chicago, IL 60637, USA
[5]Department of Pathology, Brigham and Women's Hospital, Harvard Medical School, Boston, MA 02115, USA
[6]Department of Pathology and Laboratory Medicine, Weill Cornell Medicine, New York, NY, 10021, USA
[7]Division of Pathology, Department of Translational Research and New Technologies in Medicine and Surgery, University of Pisa, Pisa, 56126, Italy
[8]University Institute of Cardiology and Pulmonology of Quebec (CRIUCPQ), Quebec City, QC G1V 4G5, Canada

[†]Co-First authors
[*]Co-Senior/Corresponding authors

Background

Prostate cancer (PC) has been historically considered immunologically "cold" due to low immune infiltration and a predominantly immunosuppressive tumor microenvironment (TME). However, this understanding is largely based on immune profiling studies of metastatic, castration-resistant prostate cancer (mCRPC) and may not apply in earlier stages of disease. Furthermore, the composition and organization of the immune microenvironment in primary PC remains poorly defined, especially in relation to Gleason score, the gold standard of pathologic PC grading.

Methods

We performed 21-marker cyclic immunofluorescence (CyCIF) on 29 radical prostatectomy samples, comprising 15 low-grade (LGG; Gleason ≤ 3+4) and 14 high-grade (HGG; Gleason ≥ 4+4) PC. This yielded over 20 million spatially resolved cells. We then detected over 500 B and T-cell immune clusters and analyzed their association with tumor grade and key T and B-cell subtypes.

Results

Across 29 prostatectomies and 99 tumor domains, we observed a paradoxical increase in tumor-infiltrating lymphocytes with higher Gleason grade. B-cell density varied ~100-fold (~5–500 cells/mm^2) and was higher in HGG than LGG PC ($p=0.006$). In HGG, B-cell density was comparable to mismatch-repair deficient colorectal cancer. CD8$^+$ T-cell density averaged 71 vs 135 cells/mm^2 in LGG vs HGG but remained ~2–5x lower than pMMR/dMMR CRC. CD4$^+$ T-cells were also increased in HGG ($p=0.046$).

We identified 257 B-cell-enriched clusters (BICs) and quantified their organization, from loose collections to organized aggregates. Our approach (ICAT) was compared against blinded expert pathology review. By either expert or quantitative analysis, morphologically mature BICs were ~4x more prevalent in HGG ($P=0.0001$) than in LGG. Ki67$^+$ B cells and CD21$^+$/CD23$^+$ follicular dendritic cells were significantly enriched in HGG. These are hallmarks of functional germinal centers and supportive of bona fide TLS-like biology within prostate tumors.

Within immune clusters, PD-1$^+$CD8$^+$ T-cells were ~5x more prevalent in HGG vs LGG ($p=2.4\times10^{-6}$), and TCF1$^+$ PD-1$^+$ T$_{PEX}$ cells were ~7x higher ($p=1.1\times10^{-6}$). Across HGG BICs, TCF1$^+$ T-cells correlated with ICAT cluster morphology scores ($P=5.42\times10^{-23}$) and positively correlated with Ki67$^+$ B-cells ($p=1.29\times10^{-8}$; $R^2=0.25$). Cytotoxic CD8$^+$PD-1$^+$GZMB$^+$ T-cells comprised up to 0.9% of all T-cells and were significantly more abundant in HGG (higher GZMB$^+$ fraction among CD8$^+$ T-cells, $P=0.002$; CD8$^+$GZMB$^+$ among all T-cells, $P=0.01$), with a trend toward closer ≤2 μm tumor contact in HGG ($P=0.068$).

Conclusions

We have identified that a subset of high-grade tumor contains abundant and well-organized immune clusters that carry the spatial and cell phenotypic hallmarks of TLSs. These tumors are further enriched in key T-cell effector subtypes suggestive of an active tumor-immune response. Since mature TLSs are increasingly recognized as positive predictive biomarkers of immunotherapy response, these data collectively suggest that subsets of patients with HG PC could be susceptible to neoadjuvant immunotherapy approaches to enhance cure rates in the high-risk setting.

Funding Acknowledgements

The study was approved by The University of Chicago’s Ethics Board, approval number STU00009126-CR0003. This work was supported by the Ludwig Cancer Research, an ASPIRE Award from The Mark Foundation for Cancer Research, NCI grants U01-CA284207 and R50-CA252138 to ZM, Finnish Cultural Foundation grant No. 211288 (Ali. A), Wong Family Foundation Award (JW), ASCO Young Investigator Award (JW); S.C. was supported by training grant T32-CA009216 (NCI) and the HMS Program in Neuroscience Award. histopathology support was provided by P30 CA06516; additional support was provided by P50-CA272390, P01-CA228696, DOD W81XWH-21-PCRP-DSA, and DOD HT94252410415.

Conflicts of Interest

P.K.S. is a cofounder and member of the Board of Directors of Glencoe Software and a member of the Scientific Advisory Board for RareCyte and Montai Health; he holds equity in Glencoe and RareCyte. P.K.S. is a consultant for Merck. J.W. has provided consulting services for Bullfrog AI Inc. E.V.A is consulting for Enara Bio, Manifold Bio, Monte Rosa, Novartis Institute for Biomedical Research, Serinus Bio, and TracerBio, hold equity in Tango Therapeutics, Genome Medical, Genomic Life, Enara Bio, Manifold Bio, Microsoft, Monte Rosa, Riva Therapeutics, Serinus Bio, Syapse, and TracerDx; editorial board in Science Advances; received funding from Novartis, BMS, Sanofi, NextPoint. A.P. is consulting for Exelixis, Tolmar Therapeutics, Janssen, Novartis and BostonGene and received research support from BMS, Clovis Oncology, Progenics, Janssen, Laekna, Astrazeneca, Xencor, Zenith, and Exelixis. The above authors declare that none of these relationships have influenced the content of this submission, and the other authors declare no competing interests.

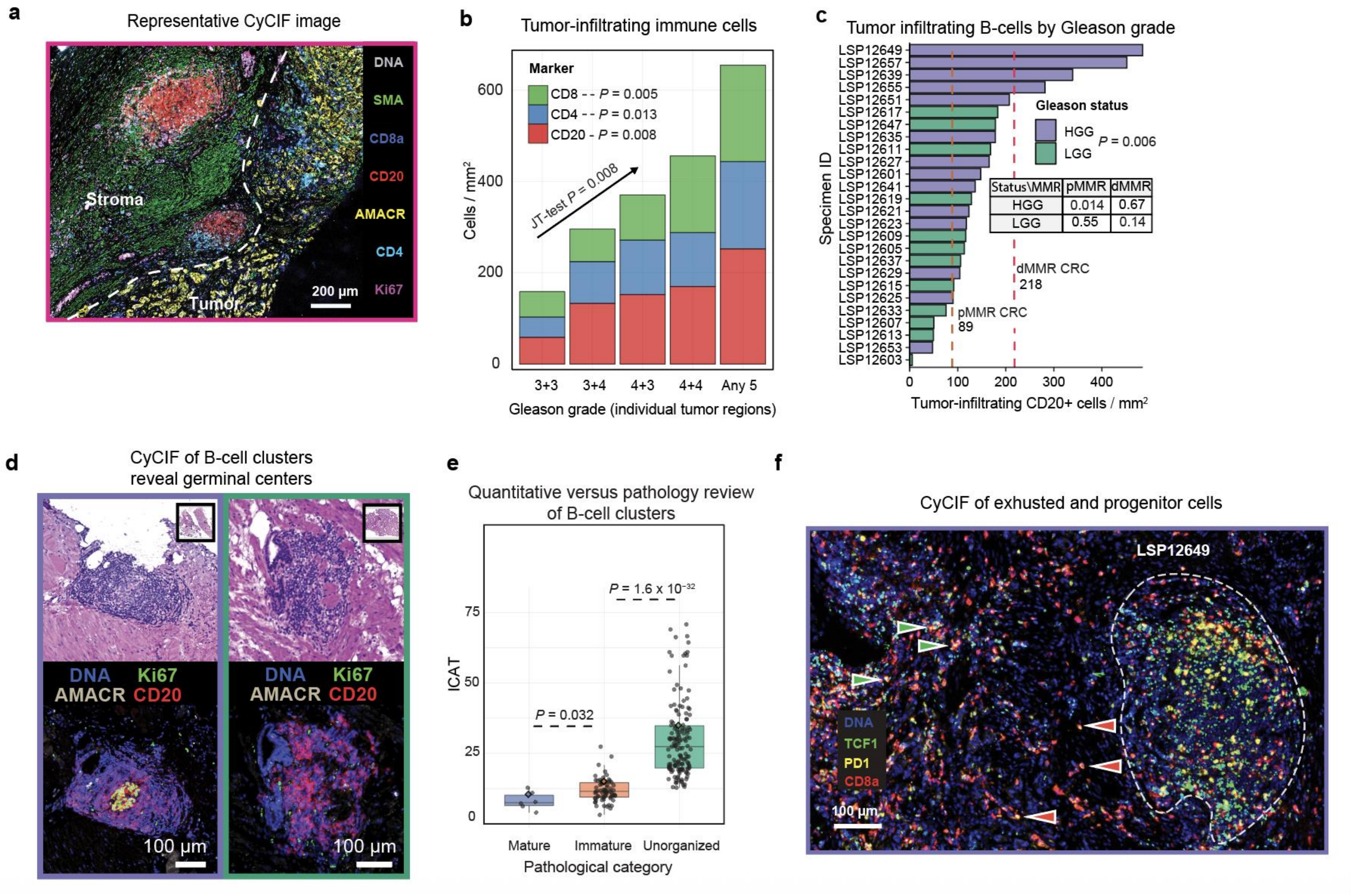

Figure 1: **a)** CyCIF image with selected markers shown; white dashed line separates the tumor and stroma compartment. **b)** Infiltration of the B cells, CD4 T cells, and CD8 T cells per mm^2 by Gleason grade **c)** Density of intratumoral CD20$^+$ T cells (cells per mm²) by Gleason grade. The one-sided Mann-Whitney U test *P* value compares high- vs low-grade disease; dashed lines indicate median reference densities in colorectal cancer as indicated. Point-wise one-sided Wilcoxon test *P* values for adjacent grade comparisons are indicated. **d)** H&E (top) and CyCIF (bottom) of exemplar BICs with (left) and without (right) a Ki67$^+$ proliferative germinal center. E) BIC ICAT scores stratified by pathologist classification. F) Representative CyCIF image highlighting increased exhaustion and progenitor-exhausted cell states adjacent to a BIC. TCF1$^+$ PD-1$^+$ CD8 T cells and TCF1$^-$ PD-1$^+$ CD8 T cells are indicated by right-pointing green arrows and left-pointing red arrows, respectively. The B-cell area is encircled by a white dashed line.